A New Method for Stranded Cable Crosstalk Estimation Based on BAS-BP Neural Network Algorithm Combined with FDTD Method

Q. Q. Liu, Y. Zhao, C. Huang, W. Yan, and J. M. Zhou

Department of Electrical and Automation Engineering
Nanjing Normal University, Nanjing, 210046, China
1376684687@qq.com, zhaoyang2@njnu.edu.cn, 1547796467@qq.com, 61197@njnu.edu.cn, 386439740@qq.com

Abstract **─** In this paper, based on the research of back propagation (BP) neural network algorithm optimized by the beetle antennae search (BAS) algorithm, a new method for predicting stranded cable crosstalk is proposed. Firstly, the stranded wire model and the equivalent multiconductor transmission lines model are both established. Then, the extraction network of the stranded wire electromagnetic parameter matrix is constructed by using the BAS-BP neural network algorithm. Finally, the network is combined with the finite difference time domain (FDTD) method to solve the near end crosstalk (NEXT) and far end crosstalk (FEXT) of a specific three-core stranded model. The new method has good agreement with the crosstalk results obtained by the electromagnetic field numerical method. The validity of the new method is verified.

Index Terms **─** Back propagation (BP) neural network algorithm, Beetle antennae search (BAS) algorithm, Finite difference time domain (FDTD) method, Multiconductor transmission lines (MTL), Stranded cable crosstalk.

I. INTRODUCTION

In the 1960s, scholars began to study the internal crosstalk of twisted pair [1]. Some scholars also studied the electromagnetic characteristics of the stranded wire in the field coupling [2-3], but the research on the internal crosstalk of multi-core stranded wire is still less. The stranded wire is realized by the equal-angle rotation of the twisted single-wire winding bobbin and the uniform forward movement of the stranded wire, which has strong anti-interference ability [4]. It is suitable for high working frequency.

Generally, the stranded wire crosstalk can be analyzed by referring to the research method of the non-uniform transmission line [5-6]. In the cascade idea proposed by Professor C. R. Paul, the cascading uniform transmission line is equivalent to a non-uniform transmission line and the per unit length (p.u.l.) RLCG electromagnetic parameter matrix can describe the transmission equation of each uniform transmission line [7-10]. The FDTD algorithm has good advantage in solving the crosstalk of non-uniform transmission lines, which is based on the cascaded transmission line theory (TLT) [11]. The most critical step in solving crosstalk by using FDTD algorithm is to extract the RLCG parameters of the transmission line. In [12], the domain decomposition method (DDM) is used to calculate the capacitance and inductance matrix of an arbitrary cross-section multiconductor transmission line (MTL). In [13], the integral equation (IE) method is used to extract the resistance parameters of random rough surface wires. In [14], the finite element method (FEM) is used to solve the problem of electromagnetic parameter extraction. In [15], the parameter matrix of the random unit length of a circular conductor is analyzed by using the polynomial chaotic coefficient. However, there is no good way to extract the electromagnetic parameters of multi-core strands.

In fact, the electromagnetic parameter matrix of the strand changes as the stranded cable changes along the extension axis. Also, the strand wire can be viewed as a multiconductor transmission line with a continuously rotating cross section at the angle of the extension axis. In order to visualize the influence of this continuous variation on the RLCG electromagnetic parameter matrix of the stranded wire, BP neural network with strong nonlinear mapping ability was introduced in our previous research to extract the RLCG electromagnetic parameter matrix at any position of the strand [16-18]. However, from a mathematical point of view, the conventional BP neural network is a local search method, which solves a complex nonlinear problem. In addition, BP neural network is very sensitive to initial network weights, and initialize network with different weights, which tend to converge to different local minimums. It is the reason why scholars get different results each time they training [19-20]. Aiming at the defect of BP neural network, this paper finally proposes an algorithm model of the BAS algorithm optimization BP neural network (BPNN). The BAS algorithm searches by the individual beetle, which has higher precision and efficiency [21]. Finally, in the solution analysis part of the crosstalk, this paper combines the stranded wire electromagnetic

Submitted On: October 17, 2019
Accepted On: December 15, 2019

parameter matrix extraction network with the FDTD algorithm to estimate the NEXT and FEXT of a specific three-core stranded wire.

Based on the BAS-BP algorithm, this paper proposes a new approach for the electromagnetic parameter extraction of the stranded wire. Then using the FDTD algorithm to calculate the NEXT and FEXT of the stranded wire. Section II defines the model of the stranded wire and the sample extraction model of the stranded electromagnetic parameters. Section III deals with the specific implementation flow of the BAS-BP neural network algorithm combined with the FDTD method. Section IV provides the analysis of a specific three-core stranded wire model by using the BAS-BP algorithm combined with the FDTD method and the verification of the crosstalk simulation. Section V summarizes this paper.

II. STRANDED WIRE MODELING

A. Establishment of the stranded wire model

For the convenience of research, only the stranded wire with the same cross-sectional shape is considered. In this paper, the stranded wire is modeled on the basis of a single spiral [22]. Figure 1 is the single spiral model. (1) and (2) are mathematical formulas for the single spiral:

$$\begin{cases} x = R_1 \sin(\alpha l) \\ y = R_1 \cos(\alpha l), \\ z = \alpha pl / 2\pi \end{cases} \tag{1}$$

$$\alpha = \sqrt{(R_1^{\ 2}) + (p/2\pi)^2}\ . \tag{2}$$

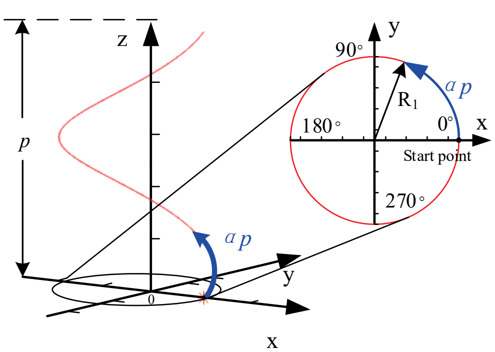

Fig. 1. Single spiral model.

Where R_1 is the radius of rotation, α is the twist factor, p is the pitch, αp is the angle of rotation, and l is the line length. In fact, the n-core strand is composed of n single wires, but the starting positions of different single wires are different. In this paper, any cross section that is consistent with the initial cross-sectional shape of the n-core strand is defined as the transposition of the n-core strand, and the adjacent transpositions are phase-shifted by $2\pi/n$. The position of the transposition corresponds to the position of the stranded line is kp/n, and the corresponding degree of radial rotation is $2k\pi/n$, where k=1, 2...n. Taking the three-core stranded wire as an example, the degree of rotation of the cross section of the transposition is $2\pi/3$, $4\pi/3$, 2π, as shown in Fig. 2.

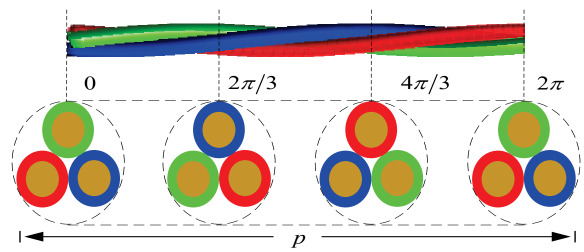

Fig. 2. Three-core stranded wire model.

B. RLCG parameter sample matrix extraction model

Stranded wires in engineering application typically contain separate insulating layers, which may also contain shielding layers. The finite element method (FEM) is able to accurately and quickly solve the p.u.l. RLCG parameter matrix of a uniform transmission line of arbitrary cross section. AnsysQ3D is a circuit parasitic parameter extraction software based on the FEM algorithm, but it cannot directly extract the RLCG parameter matrix at any position of the strand.

From the cross-section, the cross-sectional shape of the strand at any position is the same. There is only a change in the relative position between the strand and the ground. From the axial extension point of view, the stranded wire can be regarded as a multiconductor transmission line which is formed by cascading an infinite number of infinitely small cross section conductors which are continuously rotated in the axial direction. Therefore, the relative position between the strand and the ground can be converted into a corresponding rotation angle, that is, one pitch of the strand corresponds to a 360° rotation angle, and the phase difference between the adjacent two pitches is 360°. So the corresponding angle of the distance from the pitch initial end at d is $\frac{d}{p} * 2\pi$.

Any position of the stranded wire corresponds to its own RLCG parameter matrix and the corresponding rotation angle. For the unique property of the stranded wire, the p.u.l. RLCG parameter matrix of the multi-core uniform transmission line with different rotation angles can be extracted by the above simulation software. Then the sample parameter matrix required for the BAS-BP neural network and its corresponding angle matrix as the network input can be obtained.

Equation (3) is the electromagnetic parameter matrix of the n-conductor transmission line:

$$X = \begin{bmatrix} x_{11} & x_{12} & \cdots & x_{1n} \\ x_{21} & x_{22} & \cdots & x_{2n} \\ \cdot\cdot & \cdot\cdot & \cdots & \cdot\cdot \\ x_{n1} & x_{n2} & \cdots & x_{nn} \end{bmatrix}. \tag{3}$$

Where X represents the RLCG parameter matrix and x represents the specific value of the electromagnetic parameter. When the loss is not considered, the RLCG electromagnetic parameter matrix of the transmission line is a symmetric matrix, $x_{ji} = x_{ij}$. Therefore, it is only necessary to take the main diagonal element number and the upper triangular element of the matrix as the research object, as shown in the formula (4), (5):

$$\dot{R} = [r_{11}, r_{12}, r_{22}, ..., r_{nn}], \dot{L} = [l_{11}, l_{12}, l_{22}, ..., l_{nn}], \tag{4}$$

$$\dot{C} = [c_{11}, c_{12}, c_{22}, ..., c_{nn}], \dot{G} = [g_{11}, g_{12}, g_{22}, ..., g_{nn}]. \tag{5}$$

Replace $\dot{R}$, $\dot{L}$, $\dot{C}$ and $\dot{G}$ with the column vector y:

$$y = \left[\dot{R}, \dot{L}, \dot{C}, \dot{G}\right]^T = [y_1, y_2, ..., y_m]^T. \tag{6}$$

Where y represents the value of the sample element of the RLCG parameter matrix, the total number of elements in y is m, $m = 2n(1+n)$, n is the number of core. Figure 3 shows the RLCG parameter data processing procedure.

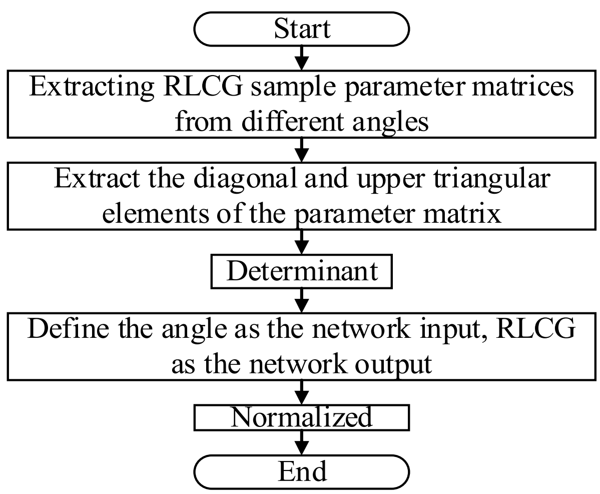

Fig. 3. Data pre-processing flow chart.

III. BAS-BP ALGORITHM COMBINED WITH FDTD ALGORITHM PREDICTING CROSSTALK

A. BP neural network algorithm

The BP network is mainly composed of signal forward propagation and error back propagation. Forward propagation is the process, by which the signal is input by the input layer and processed by the output layer after being processed by the hidden layer neurons. If the error between the predicted value and the true value does not meet the accuracy requirements set by the network, it will turn to the back propagation phase of the error. Error backpropagation is to pass the obtained error back to the input layer through the hidden layer. In this process, the error is distributed to each neuron and the weight and threshold are adjusted along the direction, in which the error function decreases the fastest. This process continues to cycle until the error in the training network output meets the accuracy requirements or the number of iterations is reached.

By analyzing the number of input and output elements, a small and medium-sized BP neural network with only one hidden layer is selected.

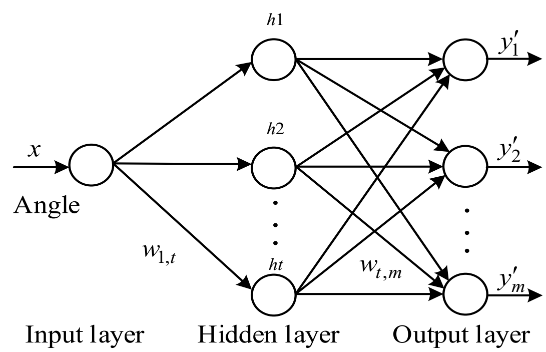

Fig. 4. Topological structure of the BP neural network.

Figure 4 is a single hidden layer BP neural network topology. The stranded wire rotation angle is the input of the network, and the RLCG parameter column vector is the network output. $w_{1,t}$ is the weight of the hidden layer from the input layer to the t-th layer, $w_{t,m}$ is the weight of the t-th layer hidden layer to the m-th layer output layer, t is the number of hidden layer neurons, and t is an empirical range value. It is affected by the number of input elements n and the number of output elements m:

$$t = 0.5(m+n) + a, (a = 1, 2, ..., 10). \tag{7}$$

B. BAS algorithm

The BAS global search algorithm [21] is a meta-heuristic algorithm for multi-objective function optimization based on the principle of the beetle foraging proposed in 2017. When the beetle is foraging, it always distinguishes the direction according to the strength of the food smell. The beetle has two long antennae. If the right side of the antenna receives stronger odor than the left side, the beetle will fly to the right, otherwise it will fly to the left. According to this simple principle, the beetle can effectively find food. Similar to genetic algorithms, particle swarm optimization, etc., the BAS algorithm can automatically implement the optimization process without knowing the specific form of the function and the gradient information. However, compared with the swarm intelligence optimization algorithm, the BAS algorithm only needs one beetle, the computational complexity is greatly reduced, and its core code is only four lines, which is easy to implement. For low-dimensional optimization functions, it has a very high convergence speed and convergence quality.

The algorithm flow is as following [20]:

(1) Establish and normalize the random vector of the beetle facing:

$$\vec{b} = \frac{rands(k,1)}{\| rands(k,1) \|}. \tag{8}$$

Where *rands*() is a random function, *k* represents the spatial dimension.

(2) Calculate the coordinates of the space position of the beetle:

$$\begin{cases} x_{rt} = x^t + d_0 * \vec{b} / 2 \\ x_{lt} = x^t - d_0 * \vec{b} / 2 \end{cases}, (t = 0,1,2,...,n). \tag{9}$$

Where x_{rt} indicates the position coordinates of the right-handed beard on the *t*-th iteration; x_{lt} indicates the position coordinate of the left-handed beard on the *t*-th iteration; x^t represents the centroid coordinate of the beetle at the *t*-th iteration; d_0 represents the distance between the left and right beard.

(3) According to the fitness function, it is confirmed that the odor intensity, that is the intensity of $f(x_l)$ and $f(x_r)$, $f()$ is the fitness function.

(4) Update the position of the beetle:

$$x^{t+1} = x^t - \sigma^t * \vec{b} * sign(f(x_{rt}) - f(x_{lt})). \tag{10}$$

Where σ^t represents the step factor at the *t*-th iteration; *sign*() is a symbolic function.

C. BAS-BP neural network combined with FDTD algorithm predicting crosstalk

The FDTD algorithm is a numerical method that uses cascaded ideas to solve the crosstalk of non-uniform transmission lines. According to the cascading idea, the strand can be decomposed into a series of uniform transmission lines of a finite number of tiny units. If assuming that the RLCG parameter matrix of each unit is a fixed value, the entire transmission line equation will be solved by iteratively solving the transmission line equation of each unit.

Figure 5 is the equivalent circuit model of the p.u.l. multiconductor transmission lines. Where *dz* represents an infinitesimal length transmission line. r_i and r_j are the p.u.l. resistors that make up the resistance matrix R. l_{ii} and l_{ij} are the p.u.l. self-inductance and mutual inductance that constitute the inductance matrix L. c_{ii} and c_{ij} are the p.u.l. self-capacitance and mutual capacitance that constitute the capacitance matrix C. g_{ii} and g_{ij} are the p.u.l. self-directed and transconducted that form the conductance matrix G.

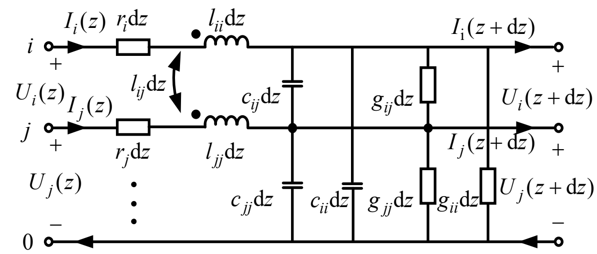

Fig. 5. The per unit length equivalent circuit for MTLs.

According to the TLT [24], the uniform multiconductor transmission line equation is:

$$\frac{\partial U}{\partial z} = -RI - L\frac{\partial I}{\partial t}, \tag{11}$$

$$\frac{\partial I}{\partial z} = -GV - C\frac{\partial V}{\partial t}. \tag{12}$$

Where *U*, *I* represent the voltage and current of the transmission line, respectively and they are a function of space *z* and time *t*. Therefore, the establishment of the multiconductor transmission line equation largely depends on the acquisition of the p.u.l. RLCG parameter matrix. In other words, the most important step in solving the stranded wire crosstalk by using the FDTD algorithm is to obtain a high-precision RLCG parameter matrix.

From a mathematical point of view, there is a highly nonlinear mapping relationship *F* between the RLCG parameters and the rotation angle (from the initial port position) in the strand model:

$$X = F(angle). \tag{13}$$

This kind of functional relationship is difficult to express with common functions, but BP neural network can describe this mapping effectively and conveniently [16]. At the same time, many existing researches show that using the optimization algorithm to optimize the BP neural network initial weights, then training the network can greatly improve the network performance. It can greatly avoid the problem that random initialization causes the network falling into local optimum. Similar to the genetic algorithm, particle swarm algorithm and other intelligent optimization algorithms, it can better solve the poor accuracy of the BP neural network. However, the above optimization algorithm occupies more computer memory, and the main program runs longer [19]. Considering the accuracy and calculation time, this paper uses the BAS global search algorithm to find the optimal initial weights and thresholds of the BP neural network, and applies it to the constructed network to construct the final training network [21]. The model constructed by this method can well overcome the problems of poor stability of the BPNN and prevent it falling into local optimum. The modeling steps are as following:

(1) Create a random vector to be oriented by the

beetle and define the spatial dimension k. The model structure is $1-M-N$. 1 is the number of neurons in the input layer (angle), M is the number of neurons in the hidden layer and the number of neurons in the output layer is N. Then the spatial dimension for searching is k, $k=1*M+M*N+M+N$.

(2) Setting of the step factor σ. The step factor is used to control the regional search ability of the beetle. The initial step size should be as large as possible to cover the current search area and not fall into the local minimum. This paper adopts the linear decreasing weight strategy to ensure the fine search:

$$\sigma^{t+1}=\sigma^{t}*eta, t=(1,2,...,n). \tag{14}$$

Where eta takes the number close to 1 between [0,1], and takes 0.8 in this paper.

(3) Determine the fitness function. The root mean square error (MSE) of the test data is used as a fitness evaluation function to advance the search for spatial regions. The function is:

$$fitness=MSE=\frac{1}{N}\sum_{i=1}^{N}(t_{sim}(i)-y_i)^2. \tag{15}$$

Where N is the number of samples for the training set; $t_{sim}(i)$ is the output value for the model of the i-th sample; y_i is the actual value of the i-th sample. Therefore, the position where the fitness function value is the smallest when the algorithm iterates to stop is the optimal solution for the problem.

(4) Initialize the beetle position. The initial parameter takes the random number between [-0.5, 0.5] as the initial solution set of the BAS algorithm, which is the initial position of the beetle, and saves it in *bestX*.

(5) Evaluation. The fitness function value at the initial position is calculated from the fitness function (15) and stored in *bestY*.

(6) Update the position of the beetle. According to the formula (9), the position coordinates of the left and right beards are updated.

(7) Updating of the solution. According to the position of the left and right whiskers in the algorithm of the beetle, the right and left fitness function values are respectively obtained. Comparing the intensity and updating the position of the beetle according to equation (10), that is, adjust the weights and thresholds of the BP neural network. Then calculating the fitness function value at the current position. If the fitness function value at this time is better than *bestY*, it should update *bestY*, *bestX*.

(8) Iterative stop control. Determining whether the fitness function value reaches the set precision (taken as 0.000005) or iterates to the maximum number (100 generations). If the condition is met, it goes to step (9). Otherwise, it returns to step (6) to continue iteration.

(9) Optimal solution generation. When the algorithm stops iterating, the solution in the *bestX* is the optimal solution of the training, that is the optimal initial weights and thresholds of the BP neural network. The above optimal solution is brought into the BP neural network for secondary training and learning. Finally, the stranded wire RLCG parameter matrix extraction model is formed.

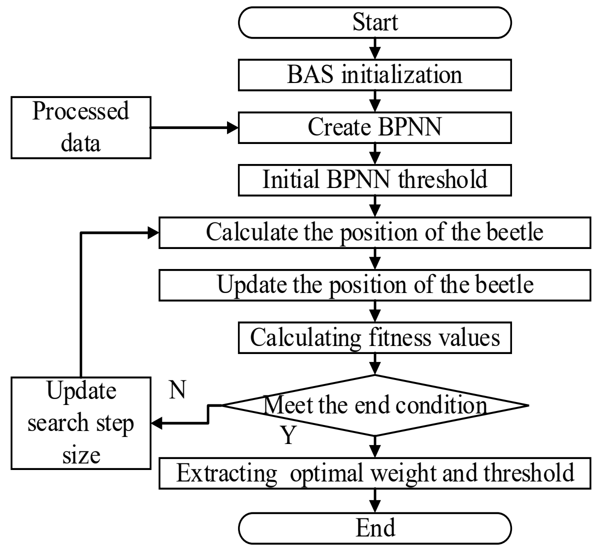

Fig. 6. The BAS algorithm optimized BP neural network flow chart.

By combining the RLCG parameter matrix extraction network at any position of the strand and the FDTD algorithm, the crosstalk of the strand can be predicted. Based on the above discussion, the specific flow chart of BAS-BP neural network model combined with FDTD algorithm for predicting crosstalk is given. Fig. 6 shows a flow chart for the BAS algorithm to optimize the initial weights and thresholds of the BP neural network. Figure 7 shows a flow chart for the BAS-BP neural network RLCG parameter extraction model combined with the FDTD algorithm to predict the stranded crosstalk.

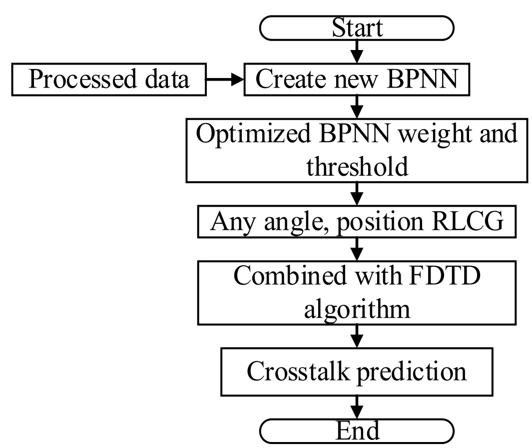

Fig. 7. The BAS-BP algorithm combines the FDTD method predicting crosstalk flow chart.

In this experiment, the BP neural network model adopts single input and single hidden layer setting. According to the empirical formula of hidden layer neurons (7), the value range of hidden layer neurons is [7,17]. In order to improve prediction accuracy, comparing the MSE values under the number of neurons in each hidden layer in turn, and select the optimal t value, that is, the number of neurons in the hidden layer is 12. Therefore, for the three-core stranded wire, the BP neural network structure is set to 1-12-12, and the dimension of the search space of the beetle search algorithm is 180. Since there are no effective guiding theories and methods for setting the step factor in the BAS algorithm, the trial and error method is used here to determine the initial step size $\delta^0 = sqrt(k)$, and the number of iterations n = 100.

IV. VERIFICATION AND ANALYSIS

A. Verification test of the BAS-BP algorithm

In order to facilitate the research, this paper uses three-core stranded wire as an example to verify and analyze the proposed method. The wire radius in the wire harness is 0.89 mm. The insulating material of the wire is a PVC material having a relative dielectric constant of 2.7. The wire thickness is 0.8 mm. The wire length is 1000mm. The wire to ground distance is 8mm. Connecting 50Ω resistors at both ends of the wire. The details are shown in Table 1. The specific distribution pattern to the ground is shown in Fig. 8.

Table 1: Three-core twisted cable

Parameters	Values
Number of cores	3
Single wire radius	0.89 mm
Single wire conductivity	58000000 S/m
Single wire insulation thickness	0.8 mm
Insulation layer relative permittivity	2.7
Pitch	1000 mm
Height	4mm

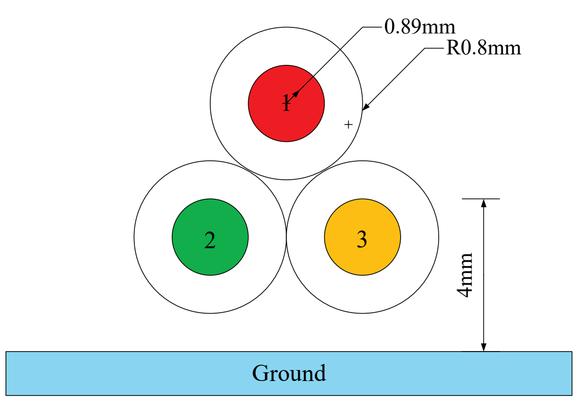

Fig. 8. Three-core stranded wire cross-section distribution pattern.

Taking the cross-section shape of Fig. 8 as the reference section (corresponding to the rotation degree of 0°), the p.u.l. RLCG parameter matrix is extracted by AnsysQ3D simulation software. Due to the axial symmetry of the three-core stranded wire, the RLCG parameter matrix in different transpositions can be transformed into each other through row-column transformation. Therefore, it is only necessary to extract the stranded RLCG parameter matrix within 1/3 of the pitch shown in Fig. 1 to obtain the RLCG parameter matrix of the entire pitch. Starting from 0° and ending at 117°, the R, L, C, G parameter matrix samples were taken from the three-core multi-stranded wire in 1/3 pitch at equal intervals of 3°to get a total of forty samples. The initial parameter matrix is as following (RLCG parameter matrix at 0°):

$$\text{R}=\begin{bmatrix} 0.365, 0.016, 0.037 \\ 0.016, 0.305, 0.009 \\ 0.037, 0.009, 0.336 \end{bmatrix}\Omega, \tag{16}$$

$$\text{L}=\begin{bmatrix} 585.44, 314.15, 314.15 \\ 314.15, 529.95, 287.82 \\ 314.15, 287.82, 529.95 \end{bmatrix}\times 10^{-9} H, \tag{17}$$

$$\text{C}=\begin{bmatrix} 62.011, -27.019, -27.026 \\ -27.019, 65.049, -25.750 \\ -27.026, -25.750, 65.068 \end{bmatrix}\times 10^{-12} F, \tag{18}$$

$$\text{G}=\begin{bmatrix} 0.875, -0.435, -0.435 \\ -0.435, 0.893, -0.434 \\ -0.435, -0.434, 0.893 \end{bmatrix}\times 10^{-3} S. \tag{19}$$

In general, the effect of the R and G parameters is ignored because the transmission line resistance is much smaller than its termination resistance. Therefore, the BAS-BP neural network only trains and tests the L and C parameter matrices of the three-core stranded wire. This experiment sets the training error accuracy of the neural network to $E_{\min} = 10^{-6}$. The BAS-BP neural network algorithm flow of Fig. 5 was used in combination with the MATLAB2018 software platform for training and testing. The samples were randomly arranged using a random function. The first 30 sets of data were used as training data and the last ten sets of data were used as test samples. The training errors of the first 30 groups are shown in Fig. 9. The pre-set accuracy requirements are achieved around 55 generations. Figure 10 is the optimal fitness curve for the BAS-BP model, which tends to be stable after 55 generations of iteration. The corresponding ten groups of samples correspond to angles of 3°, 9°, 51°, 69°, 114°, 36°, 24°, 57°, 27°, and 33°, respectively. Figure 11 is a test error distribution diagram. The maximum error of the test does not exceed 0.008 and the mean value of the test error is only 0.0013, which shows good prediction accuracy. The formula for calculating the test error using equation (6) is as following:

$$E_{test} = \frac{y' - y}{y}. \qquad (20)$$

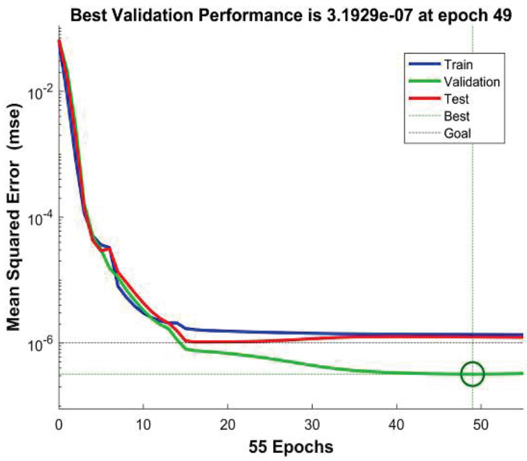

Fig. 9. The iteration number and mean square error of BAS-BP neural network training.

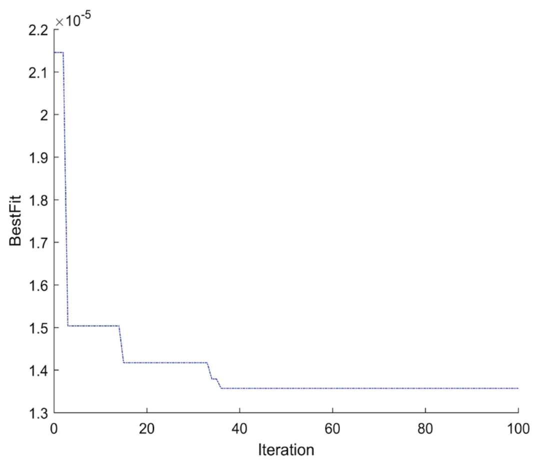

Fig. 10. The BAS-BP neural network algorithm fitness curve.

In this paper, the relative error evaluation index is selected to evaluate the performance of the model. The calculation formula is as following:

$$E_i = \frac{\left| y_i' - y_i \right|}{y_i}, (i = 1, 2, ..., n) \cdot \qquad (21)$$

Where E_i is the relative error, $y_i'(i = 1, 2, ..., n)$ is the predicted value of the i-th sample, $y_i(i = 1, 2, ..., n)$ is the true value of the i-th sample; n is the number of samples. The smaller the relative error is, the better the model performance.

In order to test whether the BAS-BP prediction model is superior to other intelligent optimization algorithm models in RLCG electromagnetic parameter extraction, this paper chooses the GA-BP neural network model and the BAS-BP model to compare prediction accuracy from relative error mean and iterative process. The performance of the model is described by the CPU running time. The results are shown in Table 2.

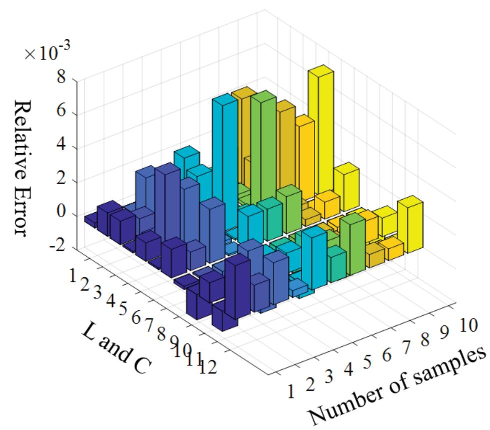

Fig. 11. Test sample error histogram.

Table 2: Comparison of different model effects

	Relative Error Mean		CPU Time/s
Model	Test L	Test C	Train
BPNN	0.0808	0.0026	0.7174
BAS-BPNN	0.0016	0.0011	39.0157
GA-BPNN	0.0023	0.0011	208.3355

It can be seen from Table 2 that the BP, the BAS-BP and the GA-BP algorithms can fit the capacitance matrix, but the accuracy of the latter two is higher than that of the BP algorithm. As to the fitting effect on the inductance matrix can be seen, the BAS-BP algorithm is optimal in extraction accuracy and the relative error mean is only 0.0016. In general, the accuracy of the BAS-BP algorithm and the GA-BP algorithm representing the optimization algorithm are not much different, but from the CPU running time, the BAS-BP is only about one-fifth of the GA-BP. Therefore, from the perspective of overall prediction accuracy and convergence speed, the BAS-BP algorithm works best, reflecting that the BAS-BP algorithm has good applicability and effectiveness in RLCG parameter extraction.

B. Crosstalk analysis

The schematic diagram of the crosstalk test of the triple-stranded wire is shown in Fig. 12. The termination is 50Ω load, ie Z_i=50Ω (where i = 1, 2, 3, 4, 5, 6), the line length is 1 meter, and the wire 1 is the power line.

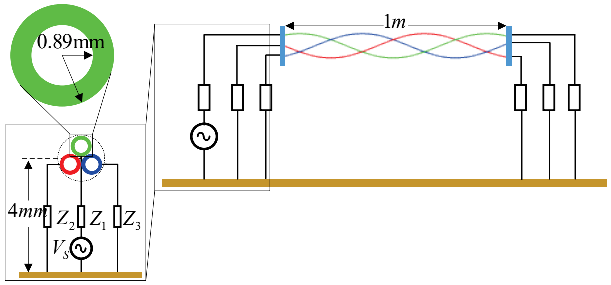

Fig. 12. Three-core stranded crosstalk experimental schematic diagram.

The stranded line RLCG parameter matrix extraction network based on the BAS-BP algorithm is combined with FDTD algorithm to predict the strand crosstalk. The crosstalk results solved by using the full wave simulation method of the CST Cable Studio® commercial software (the electromagnetic field numerical method based on the Huygens wave propagation model) were used as reference standards. The full wave algorithm is an approximate exact solution [24]. According to the parameters in Table 1, the crosstalk of the three-core stranded wire is solved by two methods in the frequency band 100KHz - 1GHz. This paper ignores the small influence of different frequencies on the electromagnetic parameters of the strand [23] and uses 500MHz as the reference value.

Figure 13 and Fig. 14 are the NEXTs of lines 2 and 3, respectively. Because of the structural characteristics of the triple-core stranded wires, the 2nd and 3rd wires have similar crosstalk characteristics. The NEXTs of lines 2 and 3 solved by the new method are both -59.17 dB at 100KHz, which are 0.68dB different from the crosstalk result of the full wave simulation, and then grow steadily in the middle and low frequency bands. At high frequencies, the NEXTs of lines 2 and 3 fluctuate around -17 dB. However, line 2 is in good agreement with the results of full wave simulation. Similarly, the FEXT results for the three-stranded strands solved by the two methods are shown in Fig. 15 and Fig. 16. The FEXTs solved by the new method are -63.30 dB at 100kHZ, which are 1dB different from the result of the full wave simulation solution, and then grow steadily in the middle and low frequency bands. At high frequencies, they fluctuate around -15 dB, and the crosstalk solved by the new method shows slight differences with full wave simulation.

By analyzing the results of the crosstalk solution, the NEXT and FEXT solved by the new method show a good agreement and consistency with the full wave simulation results, especially in the middle and low frequency bands. In the high frequency range, the new method and the full-wave simulation result do not have a slight displacement in the frequency band, but there are some discrepancies in the value, which may be caused by the following problems. First, the space segmentation of the FDTD algorithm in this paper is 150 segments, which may not achieve the actual twisting effect. In theory, as the number of segments increases, the accuracy of the new method will also increase. Second, the BAS-BP neural network constructing the stranded wire RLCG parameter extraction model still has slight deviations, and this effect will be multiplied at high frequencies. Third, for the convenience of research, this paper ignores the small influence of R, G parameters and the influence of frequency on RLCG. Fourth, the full wave simulation will affect the accuracy of the crosstalk solution because of the setting of parameters, the selection of the number of sample points, and the setting of the simulation task. It cannot perfectly reproduce the true crosstalk of the three-core stranded wire. So there is a slight impact on the consistency of two curves. However, in general, the crosstalk predicted by the BAS-BP algorithm combined with the FDTD method has extremely high precision (coincidence) at low frequencies, and at high frequencies, it is consistent with the simulation results in the trend of crosstalk.

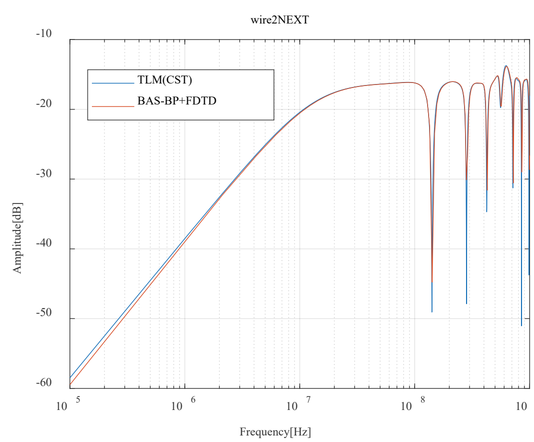

Fig. 13. Conductor No. 2 NEXT.

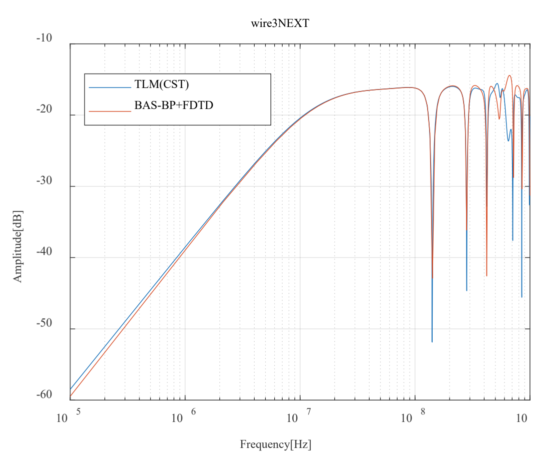

Fig. 14. Conductor No. 3 NEXT.

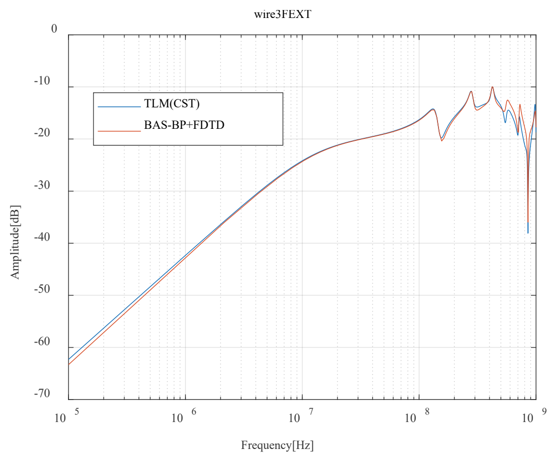

Fig. 15. Conductor No. 2 FEXT.

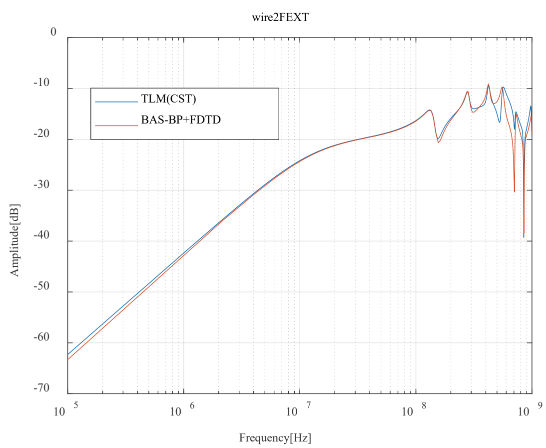

Fig. 16. Conductor No. 3 FEXT.

V. CONCLUSION

This paper proposes a new method based on the BAS-BP algorithm combined with the FDTD algorithm to predict the strand crosstalk. Through studying a specific three-core stranded wire and referring to the full wave simulation results, the applicability and high efficiency of the proposed method in the stranded wire crosstalk prediction are verified. The verification results show that, first, the RLCG parameter matrix extraction network has higher precision. The test results show that the relative error is less than 0.008 and the average relative error is only 0.0013. Second, the optimization effect of the BAS algorithm on the BP neural network is significantly better than swarm optimization algorithm. Third, in the 100KHz and 1GHz bands, the new method calculates the NEXT and FEXT of the stranded wire with high accuracy, especially in the middle and low frequency bands. Finally, the method proposed in this paper has strong vitality and creativity. There are still many places worth studying in the combination of adaptive beetle swarm algorithm and windward differential algorithm.

ACKNOWLEDGMENT

The paper is supported by National Natural Science Foundation of China (51475246), National Natural Science Foundation of Jiangsu Province (BK20161019), Aviation Science Foundation (20172552017).

REFERENCES

[1] J. R. Moser and R. F. Spencer, "Predicting the magnetic fields from a twisted-pair cable," *IEEE Transactions on Electromagnetic Compatibility*, vol. 10, no. 3, pp. 324-329, Sept. 1968.

[2] A. Y. Alksne, "Magnetic fields near twisted wires," *IEEE Transactions on Space Electronics and Telemetry*, vol. 10, no. 4, pp. 154-158, Dec. 1964.

[3] S. A. Pignari and G. Spadacini, "Plane-wave coupling to a twisted-wire pair above ground," *IEEE Transactions on Electromagnetic Compatibility*, vol. 53, no. 2, pp. 508-523, May 2011.

[4] G. Flavia, "Immunity to conducted noise of data transmission along DC power lines involving twisted-wire pairs above ground," *IEEE Transactions on Electromagnetic Compatibility*, vol. 55, no. 1, pp. 195-207, Feb. 2013.

[5] S. Grivet-Talocia, "Adaptive transient solution of non-uniform multiconductor transmission lines using wavelets," *IEEE Transactions on Antennas and Propagation*, vol. 48, no. 10, pp. 1563-1573, Oct. 2000.

[6] P. Manfredi, D. De Zutter, and D. V. Ginste, "Analysis of non-uniform transmission lines with an iterative and adaptive perturbation technique," *IEEE Transactions on Electromagnetic Compatibility*, vol. 58, no. 3, pp. 859-867, June 2016.

[7] G. Spadacini and S. A. Pignari, "Numerical assessment of radiated susceptibility of twisted-wire pairs with random non-uniform twisting," *IEEE Transactions on Electromagnetic Compatibility*, vol. 55, no. 5, pp. 956-964, Oct. 2013.

[8] C. Jullien, P. Besnier, M. Dunand, et al., "Advanced modeling of crosstalk between an unshielded twisted pair cable and an unshielded wire above a ground plane," *IEEE Transactions on Electromagnetic Compatibility*, vol. 55, no. 1, pp. 183-194, Feb. 2013.

[9] A. Shoory, M. Rubinstein, A. Rubinstein, et al., "Simulated next and fext in twisted wire pair bundles," in *Proc. EMC Europe Symp.*, York, UK, pp. 266-271, Sept. 2011.

[10] M. Tang and J. Mao, "A precise time-step integration method for transient analysis of lossy non-uniform transmission lines," *IEEE Trans-*

actions on Electromagnetic Compatibility, vol. 50, no. 1, pp. 166-174, Feb. 2018.

[11] S. Dai, A. Z. Elsherbeni, and C. E. Smith, "Non-uniform FDTD formulation for the analysis and reduction of crosstalk on coupled microstrip lines," *Journal of Electromagnetic Waves and Applications*, vol. 10, no. 12, pp. 1663-1682, June 1996.

[12] S. J. Liu, "An efficient algorithm for the parameter extraction of multiconductor transmission lines in multilayer dielectric media," *IEEE Antennas and Propagation Society International Symposium*, July 2005.

[13] Q. Chen and N. Wong, "A stochastic integral equation method for resistance extraction of conductors with random rough surfaces," in *Proc. IEEE. Int. Symp. on Intelligent Signal Processing and Communications*, Tottori, Japan, pp. 411-414, Dec. 2006.

[14] G. Plaza, F. Mesa, and M. Horno, "Quick computation of (C), (L), (G), and (R) matrices of multiconductor and multilayered transmission systems," *IEEE Transactions on Microwave Theory and Techniques*, vol. 43, no. 7, pp. 1623-1626, July 1995.

[15] P. Manfredi and F. G. Canavero, "Numerical calculation of polynomial chaos coefficients for stochastic per - unit - length parameters of circular conductors," *IEEE Trans. on Magnet.*, vol. 50, no. 3, pp. 74-82, Mar. 2014.

[16] T. Rashid, *Make Your Own Neural Network.* Charleston, USA: Create Space Independent Publishing Platform, 2016.

[17] M. Hassoun, *Fundamentals of Artificial Neural Networks*. Cambridge, USA: Bradford Book, 2003.

[18] C. Yang, et al., "Analysis on RLCG parameter matrix extraction for multi-core twisted cable based on back propagation neural network algorithm," *IEEE Access*, vol. 2, no. 1, pp. 16-19, Aug. 2019.

[19] H. L. Yang, H. C. Lin, and S. Huang, "Forecasting exchange rate using EMD and BPNN optimized by particle swarm optimization," *International Conference on Data Mining and Intelligent Information Technology Applications*, Oct. 2011.

[20] T. T. Wang and Q. Liu, "Prediction of storm surge disaster loss based on BAS-BP model," *Marine Environmental Science*, vol. 37, no. 3, pp. 457-463, 2018 (in Chinese).

[21] X. Jiang and S. Li, "Beetle antennae search without parameter tuning (BAS-WPT) for multi-objective optimization," Nov. 2017.

[22] C. D. Taylor and J. P. Castillo, "On the response of a terminated twisted - wire cable excited by a plane-wave electromagnetic field," *IEEE Transactions on Electromagnetic Compatibility*, vol. 2, no. 1, pp. 16-19, Feb. 1980.

[23] C. R. Paul, *Analysis of Multiconductor Transmission Lines.* 2nd ed., New York, USA: Wiley, 1994.

[24] CST Microwave Studio, ver. 2008, Computer Simulation Technology, Framingham, MA, 2008.